

## **A MODIFIED STRESS MODEL TO PREDICT THE ULTIMATE BENDING STRENGTH OF SOLID TIMBER BEAMS USING PLASTIC APPROACH**

**Khin Maung Zaw<sup>1</sup>, Zainai Mohamed<sup>2</sup>, Abd Latif Saleh<sup>2</sup>,  
Suhaimi Abu Bakar<sup>2</sup>**

<sup>1</sup>*Former post-graduate student at Faculty of Civil Engineering, UTM Skudai*

<sup>2</sup>*Faculty of Civil Engineering, Universiti Teknologi Malaysia Skudai, 81310 Johor, Malaysia*

---

**Abstract:** A modified stress model based on the principle of plasticity to predict the ultimate bending strength of solid timber beams was developed. The model is capable to predict the actual bending strength of timber beams better than the existing stress models. The two main controlling parameters of the model are the ultimate tensile and compressive strengths of the beam material. The proposed model was verified through a series of laboratory experiments using a local hardwood timber, Dark Red Meranti. A number of specimens consisting of 12 beams, 10 tension specimens and 15 compression specimens were tested. The ultimate bending moment from test results were compared against the proposed and existing stress models. A significant non-linear relationship exists between load and deformation of timber in both bending and compression, but the stress-strain relationship is linear in tension. The strain is distributed linearly across the beam section and the neutral axis tends to shift towards the tensional side when the beam is loaded beyond the proportional limit. Although the tensile strength of the timber is larger than its compressive strength, the modulus of elasticity in tension and compression is approximately the same.

*Keywords: timber beams, ultimate strength prediction, bending tests*

**Abstrak:** Satu model tegasan diubah suai berpandukan prinsip plastik bagi penganggaran kekuatan lentur muktamad rasuk kayu padu telah dibangunkan. Model ini berupaya menganggar kekuatan lentur sebenar rasuk kayu dengan lebih tepat berbanding model tegasan sedia ada. Dua parameter kawalan bagi model ini adalah kekuatan tegangan dan kekuatan mampatan muktamad bahan rasuk. Pengesahan model yang dicadangkan telah dilakukan melalui satu siri ujian makmal menggunakan kayu keras tempatan, Meranti Merah Tua. Sebilangan spesimen yang terdiri daripada 12 rasuk, 10 spesimen tegangan dan 15 spesimen mampatan telah digunakan dalam ujian makmal. Moment lentur muktamad daripada keputusan ujian dibandingkan dengan model tegasan yang dicadangkan dan model tegasan sedia ada. Keputusan ujian makmal mendapati wujud hubungan tidak linear yang ketara di antara beban dan ubah bentuk kayu dalam lenturan dan mampatan, sebaliknya hubungan tegasan-terikan adalah linear dalam tegangan. Taburan terikan teragih secara linear pada sepanjang keratan rasuk dan paksi nutral cenderung untuk beranjak ke bahagian tegangan rasuk pada ketika rasuk dibebani dengan beban melepasi had kadaran. Walaupun kekuatan tegangan kayu lebih besar daripada kekuatan mampatan, modulus elastik dalam tegangan dan mampatan didapati hampir sama.

*Kata kunci: rasuk kayu, ramalan kekuatan muktamad, ujian lenturan*

## 1.0 Introduction

Plastic theory has been applied quite successfully in the analysis of flexural strength of reinforced concrete and steel structures. In the analysis of reinforced concrete beam sections, the actual parabolic compressive stress distribution is simplified as an equivalent rectangular stress distribution (plastic stress distribution). Similarly, steel beam sections are also analysed using plastic stress distribution for both tension and compression parts. It is possible to obtain the plastic stress distribution from ductile materials, such as steel which behaves as a perfectly plastic material. However, the linear stress distribution (elastic stress distribution) has been used in the analysis of timber beam sections although timber shows some limited ductility in bending and axial compression.

The actual flexural stress distribution pattern of a timber beam section at the failure stretch is very complex. To simplify this complexity, various modified mathematical stress models have been developed. The accuracy of the model outcome would depend upon how close the assumed model to the true stress distribution. Plasticity models for timber beam sections had been studied by many researchers (e.g. Moe, 1961; Nwokoye, 1972; Zakic, 1973; Bazan, 1980; Buchanan, 1990). Most of the researchers introduced different forms of compressive stress distribution with a triangular tensile stress distribution pattern.

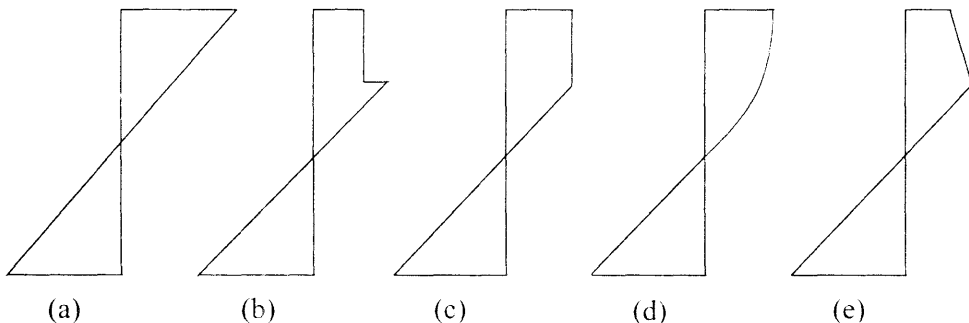


Figure 1: Existing stress models for timber beams: (a) Elastic Stress Model; (b) Moe's Stress Model; (c) Nwokoye's Stress Model; (d) Zakic's Stress Model; (e) Stress Model by Bazan and Buchanan

In this study, a modified stress model is proposed to predict the ultimate bending strength of solid timber beams using both primary and secondary research data as inputs. Compared to the previous stress models, the modification was made by introducing an additional parabolic-shaped stress distribution to increase the area of compressive stress distribution. Using the experimental data, the results predicted by the model were compared with that obtained from the existing models. A new parameter called moment coefficient ( $\psi$ ) was introduced in the newly modified model. It is derived from the equations of the stress models by using the strength ratio ( $n$ ) of the ultimate and compressive strengths of the beam material.

## 1.1 Existing Stress Models

The traditional strength analysis of a timber beam is done using classical elastic method with the assumption that the shape of the stress distribution diagram is as shown in Figure 1(a). According to the elastic stress model, ultimate tensile,  $F_{tu}$  in the top and compressive stresses,  $F_{cu}$  in the bottom of the fibres are assumed equal at failure. It means that the ratio of tensile stress to compressive stress,  $n$ , is equal to 1. So, the neutral axis is at the mid-depth of the beam section, i.e.,  $\gamma = 0.5$ , and both stress and strain are linearly distributed up to the failure point. According to classical elastic stress model, the elastic moment capacity ( $M_{elastic}$ ) of the timber beam can be described as,

$$M_{elastic} = \frac{1}{6} F_{cu} b h^2 \quad (1)$$

Moe (1961) assumed that the compressive stress distribution of a timber beam section at failure should be rectangular from compression edge to some depth where the stress immediately increased to the maximum compressive stress ( $F_{cu}$ ) as shown in Figure 1(b). Then, it decreased linearly passing through the neutral axis. However, the shape of tensile stress distribution is still triangular and linear up to the failure and the neutral axis is no longer positioned at the mid-depth of the beam at failure. Moe (1961) also assumed that modulus of elasticity is the same for tension and compression, and the ultimate tensile stress ( $F_{tu}$ ) at failure is greater than the ultimate compressive stress ( $F_{cu}$ ). The ultimate moment capacity ( $M_u$ ) of a timber beam, according to Moe's stress model, can be derived as,

$$M_u = \frac{1}{6} F_{cu} b h^2 [c\alpha(4-\alpha) + (1-\alpha)^2] \quad (2)$$

Nwokoye (1972) proposed that the shape of the compressive stress distribution at the failure of a timber beam should be a trapezoidal shaped as shown in Figure 1(c), and the position of the neutral axis is not at the mid-depth of the beam. Nwokoye also assumed that modulus of elasticity for tension and compression is the same, but the ultimate tensile stress at failure is greater than the ultimate compressive stress. He agreed that the shape of the tensile stress distribution is triangular and linear up to failure. According to Nwokoye's stress model, the ultimate moment capacity ( $M_u$ ) of the beam can be determined as,

$$M_u = \frac{1}{6} F_{cu} b h^2 \frac{(3n-1)}{(n+1)} \quad (3)$$

Zakic (1973) assumed that the stress diagram for compressive zone of a timber beam at failure is a second-degree parabolic shaped and the neutral axis

is not position at the mid-depth of the beam as shown in Figure 1(d). The ultimate tensile stress is greater than the ultimate compressive stress in the beam section. Like other researchers, he assumed that the shape of the tensile stress distribution is triangular and linear up to failure. The ultimate moment capacity ( $M_u$ ) of the beam in Zakic's stress model can be expressed as,

$$M_u = \frac{1}{6} F_{cu} b h^2 \left[ \frac{22.5 n^2 + 32n}{(3n+4)^2} \right] \tag{4}$$

Bazan (1980) adopted the bi-linear stress model as shown in Figure 1(e). This model assumed the same modulus of elasticity for tension and compression. It is obvious that strain softening was considered in this plasticity model for compressive stress-strain relationship. However, like other researchers, he assumed the tensile stress distribution to be triangular and linear up to failure. He also agreed that the ultimate tensile stress ( $F_{tu}$ ) is greater than the ultimate compressive stress ( $F_{cu}$ ) by a factor of  $n$ , which is greater than 1. According to Bazan's stress model, the ultimate moment capacity ( $M_u$ ) of the beam can be derived as,

$$M_u = \frac{1}{6} F_{cu} b h^2 \frac{(3n)}{(n+2)} \tag{5}$$

Buchanan (1990) also assumed a bi-linear model with some similarity to the model proposed by Bazan (1980). Unlike Bazan, Buchanan (1990) proposed that the relationship between the reducing stress,  $F_{cu}(1 - c)$ , and the increasing strain,  $(\epsilon_c - \epsilon_o)$ , is directly related to the slope ( $m$ ) of the falling branch of the modulus of elasticity in modified compressive stress-strain curve. The ultimate moment capacity ( $M_u$ ) of the beam, according to Buchanan's stress model can be described as,

$$M_u = \frac{1}{6} F_{cu} b h^2 \left[ \frac{n + c(2n - 1)}{(n + c)} \right] \tag{6}$$

$$c = \sqrt{1 - m(n^2 - 1)} \tag{7}$$

## 1.2 Some Observations on Existing Stress Models

All existing stress models quoted in this paper assumed triangular tensile stress distribution regardless of different compressive stress distributions. The models used direct tension and compression test results to predict the strength of timber beams. Except elastic stress model, all other model had been developed based on non-linear nature of timber in compression through the fact that timber is stronger in tension than in compression. The elastic model ignored the non-linear behaviour of wood in compression and, hence, under-

estimated the strength of timber beams. Stress models developed by Moe (1961) and Buchanan (1990) are difficult to utilise because they require additional parameters, i.e. compressive strength reduction factor ( $c$ ) for Moe's stress model and the slope ( $m$ ) of the falling branch from modified stress-strain curve in axial compression for Buchanan's stress model.

## 2.0 Development of the Modified Stress Model

### 2.1 Theoretical Assumptions

In developing a modified version of stress, the following assumptions are made,

- a) Strain is linearly distributed across the section of the timber beam under bending condition up to failure and, hence, plain sections before bending remain plain after the bending.
- b) Strength ratio ( $n$ ) of axial tensile strength to axial compressive strength is greater than 1 so that the beam fails in compression first.
- c) Ultimate tensile strength ( $F_{tu}$ ) and ultimate compressive strength ( $F_{cu}$ ) are determined from structural-sized timber specimens.
- d) The stress distribution across the beam depth is linear up to the proportional limit stress in bending, beyond which the stress distribution formed a pattern as shown in Figure 2 (c).

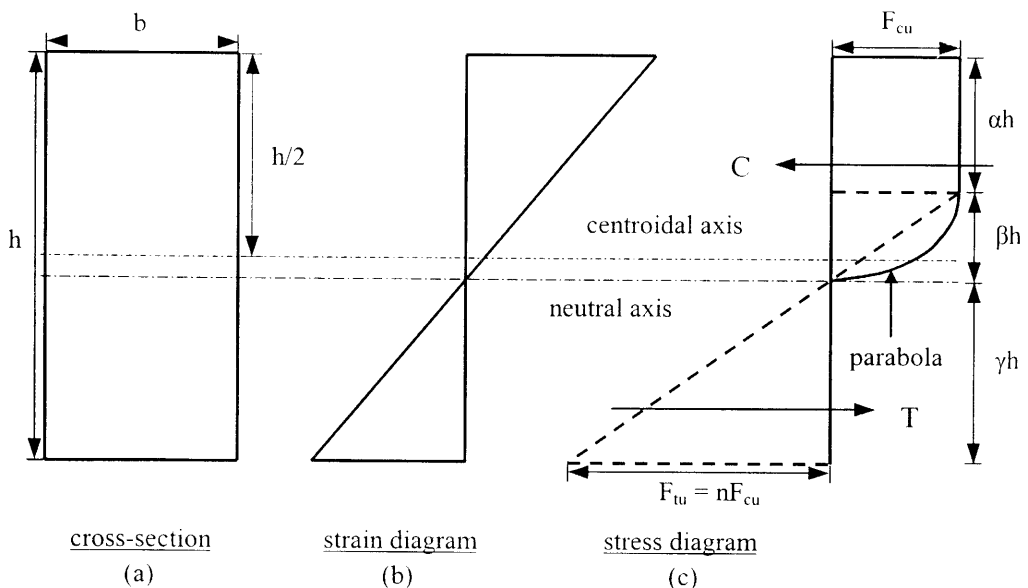


Figure 2: The theoretical stress distribution pattern

### 2.2 Formulation of the Stress Model

The current stress model was modified from the work done by Nwokoye (1972) where a trapezoidal compressive stress distribution was assumed. The

modification was made by introducing an additional parabolic-shaped stress distribution in order to increase the area of compressive stress distribution (see Figure 2c). Hence, the compressive stress distribution at the ultimate moment of the proposed model is a combination of a rectangular stress block and a second-degree parabolic stress block with its axis lying along the lower edge of the rectangular block. The origin or the vertex of the parabola is at the lower right corner of the rectangle. The area of the parabola is equal to two-third the area of the enveloped rectangle. The triangle at the base of the rectangle, shown by the dotted line, is similar in shape of the triangle representing the tension stress block. The stress distribution in the cross-section of the beam just before the failure must satisfy the following equilibrium conditions.

- a) Internal compressive force ( $C$ ) = Internal tensile force ( $T$ )
- b) Internal resisting moment = External bending moment ( $M_u$ )

Considering the stress distribution shown in Figure 2, the resultant internal compressive and tensile forces are,

$$C = F_{cu} b \alpha h + \frac{2}{3} F_{cu} b \beta h \tag{8}$$

$$T = \frac{1}{2} n F_{cu} b \gamma h \tag{9}$$

Substituting equations (8) and (9) into equilibrium condition (i) yields,

$$F_{cu} b \alpha h + \frac{2}{3} F_{cu} b \beta h = \frac{1}{2} n F_{cu} b \gamma h \tag{10}$$

$$\alpha + \frac{2}{3} \beta = \frac{1}{2} n \gamma \tag{11}$$

From the geometry of the stress distribution diagram shown in Figure 2,

$$\alpha = 1 - \beta - \gamma \tag{12}$$

$$\beta = \gamma \frac{F_{cu}}{n F_{cu}} = \frac{\gamma}{n} \tag{13}$$

From equation (11) to (13),  $\gamma$  can be expressed in terms of  $n$  as follows:

$$\gamma = \frac{6n}{3n^2 + 6n + 2} \tag{14}$$

From equations (12) to (14), expressions for  $\alpha$  and  $\beta$  can be written in terms of  $n$ :

$$\alpha = \frac{3n^2 - 4}{3n^2 + 6n + 2} \tag{15}$$

$$\beta = \frac{6}{3n^2 + 6n + 2} \tag{16}$$

According to equilibrium condition in (ii), external bending moment ( $M_u$ ) is equal to internal resisting moment, which is computed by taking moments of forces about the neutral axis:

$$M_u = F_{cu} b h^2 \left[ \alpha \left( \beta + \frac{\alpha}{2} \right) + \frac{2}{3} \beta \left( \frac{5}{8} \beta \right) + \frac{1}{2} n \gamma \left( \frac{2}{3} \gamma \right) \right] \tag{17}$$

Substituting the values of  $\alpha$ ,  $\beta$  and  $\gamma$  from equations (14) to (16) into equation (17),

$$M_u = \frac{1}{6} F_{cu} b h^2 \frac{27n^4 + 72n^3 + 36n^2 - 6}{9n^4 + 36n^3 + 48n^2 + 24n + 4} \tag{18}$$

$M_u$  from equation (18) can be expressed in the form of elastic moment [ $M_{elastic}$  in equation (1)] by multiplying with the moment coefficient ( $\psi$ ) as follows:

$$M_u = \psi M_{elastic} \tag{19}$$

where

$$\psi = \frac{27n^4 + 72n^3 + 36n^2 - 6}{9n^4 + 36n^3 + 48n^2 + 24n + 4} \tag{20}$$

$$M_{elastic} = \frac{1}{6} F_{cu} b h^2$$

### 3.0 Materials and Test Procedures

Dark Red Meranti (DRM) was chosen as the material for test specimens. DRM is a tropical hardwood timbers and most commonly used in construction in Malaysia. It is classified as a light hardwood with an average density of 730 kg/m<sup>3</sup> and specific gravity of 0.47 at 19% moisture content (Choo and Lim, 1983). According to the latest Malaysian Standard MS 544: Part 2: 2001 (2001), it is under the strength group S.G. 5 and the mean value of modulus of elasticity (MOE) 11200 MPa at moisture content 19%. Standard structural grade stresses at moisture content 19% for DRM were described as 14.3

MPa for bending, 8.6 MPa for tension parallel to grain, 11.0 MPa for compression parallel to grain.

Five large pieces 100 mm x 150 mm x 380 mm of Dark Red Meranti timber obtained from a forest at Bandar Tenggara, Johor, were selected. The specimens were previously kept to dry naturally in room temperature and natural humidity for about three years. The specimens were labelled A, B, C, D and E and each specimen was then cut into three different portions to be used in bending, tension and compression tests.

### 3.1 Bending Tests

Beam specimens were fabricated into two different cross-sections with the same length according to ASTM standard (D 198-84) (1992). FA, FB, FC, FD and FE group beams were cut from each pieces A, B, C, D and E. There were three 50 mm x 100 mm x 2100 mm beams fabricated for each of group FA and FB and two 50 mm x 150 mm x 2100 mm beams for each of group FC, FD and FE. All beam specimens were prepared in order to get 225 mm overhang on each end of the span.

The arrangement of beam test set-up is shown in Figure 3. Four 50 mm Omega strain gauges and four 100 mm Omega strain gauges were attached alternately to two opposite sides at the centre of the specimen by screwing to the small solid brass fixing jigs, which were glued to the specimen using 5-minute fast drying epoxy glue. The spacing between each strain gauge is 24 mm for 50 mm x 100 mm beams and 38 mm for 50 mm x 150 mm beams. Three Kyowa displacement transducers (LVDT) were placed directly beneath the mid span and two loading points of the beam. A Kyowa load cell was placed between the hydraulic jack and the load distributor to capture load readings. Strain gauges, displacement transducers and the load cell were connected to the data-logger to capture the readings throughout the test.

The strain for the specified depth was calculated from the average readings of the two strain gauges at the same depth on opposite sides of the beam. After the tests, the beam specimen was cut near the middle span into three 50 mm x 50 mm pieces of 25 mm thickness for moisture content and density tests. The average values were used to represent the actual moisture content and density value of the specimen.



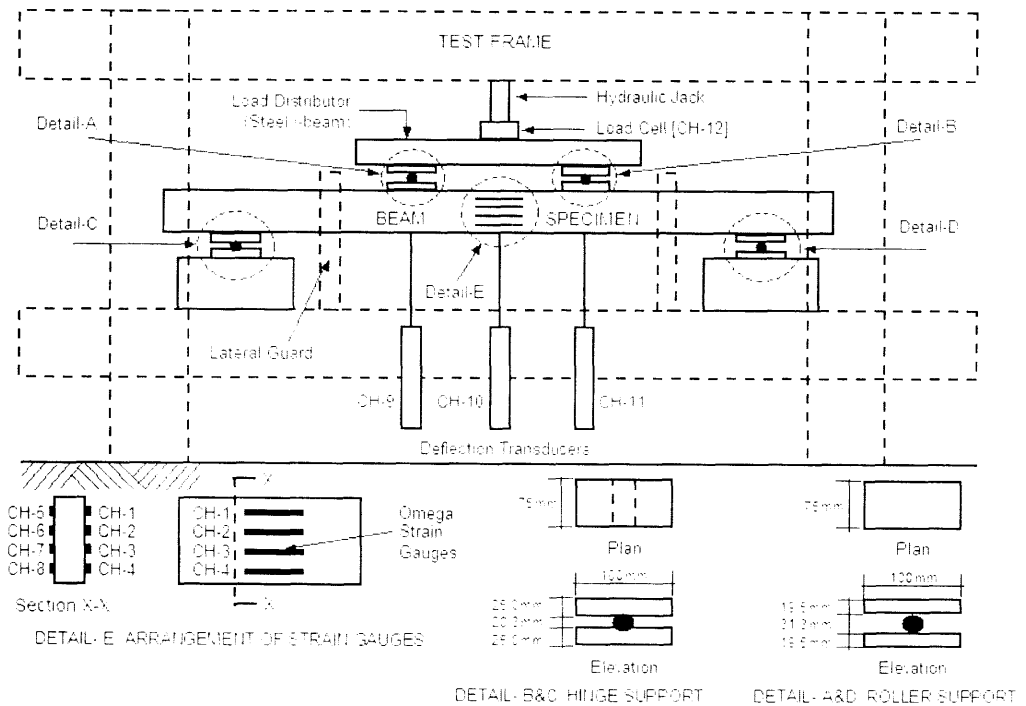


Figure 3: Schematic diagram of beam test set-up

### 3.2 Tension and Compression Tests

Tension test specimens were fabricated according to five different groups TA, TB, TC, TD and TE, cut from timber pieces A, B, C, D and E. Each group contained two 800 mm long tension test specimens, with 200 mm grip length and 400 mm in the middle including 250 mm gauge length. The nominal cross sectional dimensions of specimens were 50 mm x 25 mm within the grip length and 25 mm x 25 mm within the gauge length. Compression test specimens were also fabricated into five different groups CA, CB, CC, CD and CE cut from the same pieces of timber. The sizes of specimens were chosen based on the dimensions specified by ASTM standard (D 198-84). Each group contained three 50 mm x 50 mm x 150 mm compression specimens.

The 5000 kN Dartec universal testing machine with 250 kN loading head and wedge grips was used for tension tests, and the 250 kN Dartec universal testing machine with a swivel loading head was used for compression tests. Two 100 mm Omega strain gauges for tension tests and two 50 mm Omega strain gauges for compression tests were attached to opposite sides of the specimen by screwing to two small solid brass fixing jigs. The jigs were glued to the specimen using 5-minute fast drying epoxy glue.

The strain was calculated from the average of two strain gauge readings and the stress from the corresponding load divided by the cross sectional area

of the specimen. After the tests, three 25 mm thick pieces were cut from each specimen for moisture content and density tests according to ASTM standards (D 2395-83) and (D 4442-92) procedures. The average values were used to represent the actual moisture content and density value of the specimen.

#### 4.0 Results and Discussion

##### 4.1 Beam Tests

The beams test has shown a typical bending failure pattern under one-third-point loads. After the applied load passed the proportional limit, the beams started to fail in compression as indicated by wrinkles on the compression edge and producing some noises. The wrinkles occurred between the maximum moment region and extended from the upper compression edge to slightly more than one-half of the beam depth. A further loading beyond the proportional limit has caused the compressive stresses across the beam depth redistributed and the shifting of neutral axis towards the tension edge.

The load-deflection curves of the beams (Figure 4) are plotted using the deflection data at the mid span of the beams. The curves show that the beams are stressed well beyond the proportional limit. The curves can be divided into two different portions, i.e. linear portion (elastic stage) and non-linear portion (inelastic stage) with a rising slope. Non-linear portion of the curve occupies a significant amount (over 50%) of total deflection for most of the specimens tested.

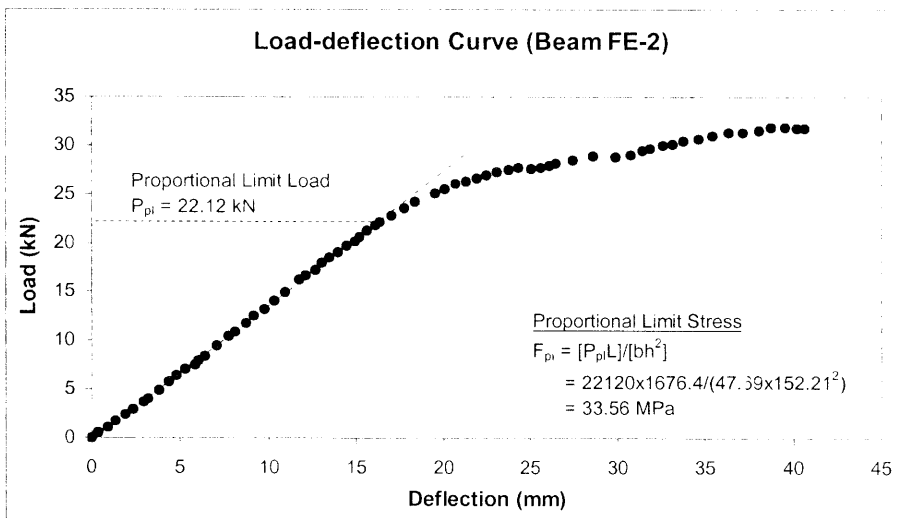


Figure 4: Typical load-deflection curve for timber beams

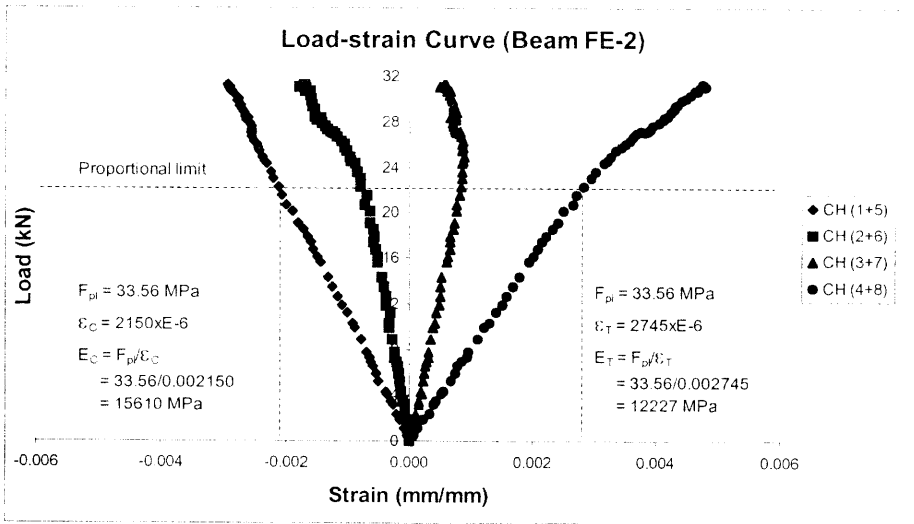


Figure 5: Typical load-strain curve for timber beams

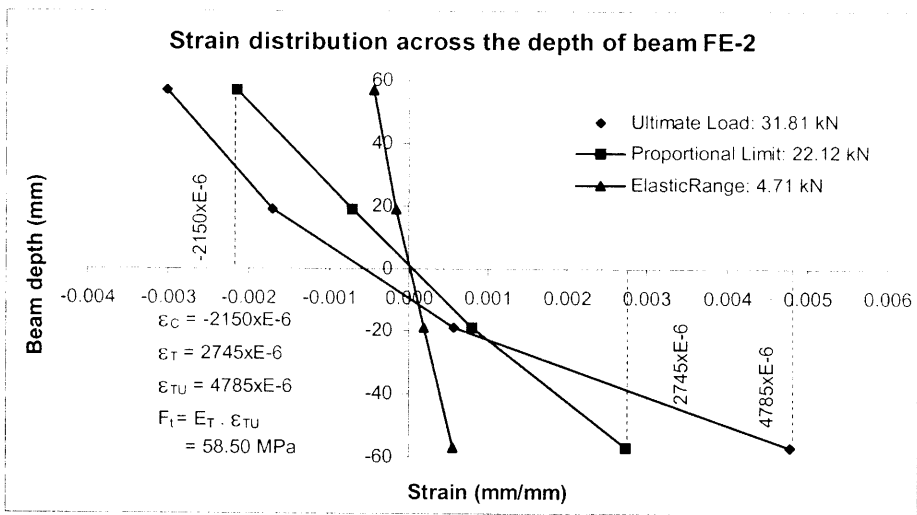


Figure 6: Typical strain distribution diagram for timber beams

Figure 5 is the load-strain curves of the beam drawn using average data from eight strain gauges. The curves show a non-linear relationship between loads and strains under inelastic condition. As a result of the downward movement of neutral axis and the redistribution of compressive stresses, tension fibres are subjected to relatively increased tensile stresses to maintain the equilibrium of the beam. These increases in stress are no longer proportional to the load on the beam.

Figure 6 is the strain distribution diagrams across the beam depth that was developed from three different loading stages: the elastic stage, the proportional limit stage and the inelastic stage at ultimate load. Linear distributed strains across the beam depth were observed in all loading stages. Deviation of strain from the linear distribution in some cases, especially at the

ultimate loading stages, may be due to the wrinkles, which appeared near mid span during the inelastic range of loading and has interfered with the action of strain gauges.

Table 1 presents the summary of beam test results. It was observed that when the applied load is small or within the elastic range, the initial position of neutral axis was slightly above or below the mid-depth of the beam. At the proportional limit load, the position of neutral axis still remained in the same position as in the elastic range. Then the neutral axis moved towards the tension edge of the beam until the ultimate load was reached. The position of neutral axis was described as the neutral axis position factor ( $\gamma$ ).

Table 1: Summary of beam test results

Beam Label	[ $E_c$ ] (MPa)	[ $E_c$ / $E_f$ ]	[ $E_f$ ] (MPa)	At Proportional Limit Load				At Ultimate Load			
				[ $F_{pl}$ ] (MPa)	[ $\epsilon_c$ ] ( $\times 10^{-6}$ )	[ $\epsilon_f$ ] ( $\times 10^{-6}$ )	[ $\gamma_{pl}$ ]	[ $M_u$ ] (kN-m)	[ $\epsilon_{ff}$ ] ( $\times 10^{-6}$ )	[ $F_f$ ] (MPa)	[ $\gamma_u$ ]
FA-1	13913	0.91	15363	39.79	2860	2590	0.49	3.65	2960	45.48	0.34
FA-2	15069	0.95	15809	30.59	2030	1935	0.45	2.33	1970	31.14	0.45
FA-3	14941	1.03	14463	38.47	2575	2660	0.50	3.88	4575	66.17	0.44
FB-1	16308	0.93	17592	41.34	2535	2350	0.49	5.49	5270	92.71	0.41
FB-2	19911	1.18	16909	48.78	2450	2885	0.48	5.68	5555	93.93	0.40
FB-3	20982	1.23	17119	40.92	1950	2390	0.49	5.56	5585	95.61	0.40
FC-1	20880	0.93	22343	54.18	2595	2425	0.49	14.77	6195	138.42	0.45
FC-2	18371	1.02	18024	47.76	2600	2650	0.49	12.47	5800	104.54	0.46
FD-1	24003	1.24	19409	49.69	2070	2560	0.50	13.45	5290	102.67	0.45
FD-2	12614	0.84	14970	47.68	3780	3185	0.47	12.15	5840	87.42	0.36
FE-1	14330	1.11	12910	28.02	1955	2170	0.49	6.25	3140	40.54	0.45
FE-2	15610	1.28	12227	33.56	2150	2745	0.49	8.89	4785	58.50	0.44

The proportional limit stress ( $F_{pl}$ ) of the beam was estimated from the load-deflection curves in Figure 4. First, a straight line was drawn passing through the points within the linear portion of the curve. Then the point of inflection was defined as the proportional limit load ( $P_{pl}$ ). The proportional limit stress ( $F_{pl}$ ) was calculated from the proportional limit load, the moment arm and the section properties of the beam.

Assuming that there is a linear stress-strain relationship for extreme tension fibres of the beams, the extreme fibre tensile stress ( $F_f$ ) is calculated from the MOE of extreme tension fibres ( $E_f$ ) and the maximum tensile strain ( $\epsilon_{ff}$ ) (Figure 6). The MOE of extreme tension fibres ( $E_f$ ) is calculated by dividing the proportional limit stress ( $F_{pl}$ ) with the tensile strain at proportional limit ( $\epsilon_c$ ), which corresponds to the proportional limit load ( $P_{pl}$ ) (Figure 5).

The ultimate bending strengths are predicted from the tension and compression test results by using the proposed stress model. The predicted strengths are compared with the actual bending strengths of the beams.

#### 4.2 Comparison between Theoretical and Experimental Results

The proposed stress model is compared with other existing stress models by means of the experimental results. However, stress models by Moe (1961) and Buchanan (1990) were not included as these models require more parameters (see Section 1.2). Table 2 presents the summary of the result. Figure 7 shows the comparison of stress models using theoretical and experimental moments. It is obvious that all the stress models under-predicted the ultimate strength of DRM timber beams. Compared to the experimental results, the elastic stress model is the most conservative with mean and standard deviation of -39.57% and 0.05, respectively. The trend line shows linear correlation between the predicted and experimental moments but lies far below the ideal line. Other stress models by Nwokoye (1972), Zakic (1973) and Bazan (1980) also under-predicted the actual strength of the beams by more than 20%. The variation of the test data, i.e. standard deviation is about the same as those predicted by elastic stress model. Their trend lines also show linear correlation and lie below but closer to the ideal line than that of the elastic stress model. By comparing with other stress models, the new stress model closely under-predicted the ultimate moment with the mean of -18.10% and the standard deviation of 0.07. The linear trend line of the new model also lies nearest to the ideal line compared with other stress models.

Of all the five models discussed above, the elastic stress model consistently under-predicts the ultimate strength of timber beams. It is because the model assumes the elastic stress distribution for the ultimate strength of timber beams, which is obviously not behaving as an elastic beam at ultimate load. The other three existing models, especially Nwokoye's and Zakic's models, also under-predicted the strength of beams but much closer to the experimental results than the elastic model. However, as summarised in Table 2 and Figure 7, the newly modified stress model is capable to better predict the ultimate strength of timber beams.

Table 2: Comparison of ultimate moments ( $M_u$ ) for stress models

Beam Label		FA-1	FA-2	FA-3	FB-1	FB-2	FB-3	FC-1	FC-2	FD-1	FD-2	FE-1	FE-2
Experimental Results	$F_{cu}$	29.34		41.75			46.66		45.59		28.27		
	$F_{tu}$	46.43		56.22			53.62		59.69		47.01		
Elastic	$n$	1.58		1.35			1.15		1.31		1.66		
	$M_{elastic}$	3.65	2.33	3.88	5.49	5.68	5.56	14.77	12.47	13.45	12.15	6.25	8.89
Stress Model	%Difference	-40.28	N.A.	-43.27	-42.64	-44.18	-42.80	-41.75	-30.92	-37.79	-30.61	N.A.	-41.44
Nwokoye's	$M_u$	3.16	3.17	3.19	4.09	4.12	4.13	9.80	9.82	10.61	10.69	7.38	7.79
Stress Model	%Difference	-13.44	N.A.	-17.76	-25.56	-27.55	-25.76	-33.62	-21.28	-21.09	-11.98	N.A.	-12.38
Zakic's	$M_u$	3.05	3.06	3.08	4.09	4.12	4.13	10.32	10.33	10.72	10.80	7.04	7.43
Stress Model	%Difference	-16.56	N.A.	-20.74	-25.47	-27.46	-25.67	-30.14	-17.16	-20.33	-11.13	N.A.	-16.40
Bazan's	$M_u$	2.89	2.90	2.91	3.81	3.83	3.85	9.42	9.43	9.94	10.01	6.71	7.08
Stress Model	%Difference	-20.93	N.A.	-24.89	-30.66	-32.51	-30.84	-36.20	-24.34	-26.13	-17.61	N.A.	-20.32
New Stress Model	$M_u$	3.25	3.26	3.28	4.24	4.27	4.28	10.31	10.32	11.04	11.12	7.56	7.99
Model	%Difference	-11.03	N.A.	-15.48	-22.74	-24.81	-22.95	-30.22	-17.25	-17.93	-8.45	N.A.	-10.18

% Difference of $M_u$ in terms of =>	Mean	Standard Deviation
Elastic Stress Model	-3956.70%	4.96
Nwokoye's Stress Model	-2104.12%	7.22
Zakic's Stress Model	-2110.68%	5.97
Bazan's Stress Model	-2644.38%	5.98
New Stress Model by KMZ	-1810.20%	7.07

$M_u$  : Ultimate moment (kN-m)  
 $M_{elastic}$  : Elastic moment (kN-m)  
 $F_{cu}$  : Ultimate compressive stress averaged from compression tests  
 $F_{tu}$  : Ultimate tensile stress averaged from tension tests (MPa)  
 $n$  : Strength ratio ( $F_{tu}/F_{cu}$ )  
 % Difference :  $\{(\text{Predicted } M_u - \text{Experimental } M_u) / \text{Experimental } M_u\} \times 100\%$

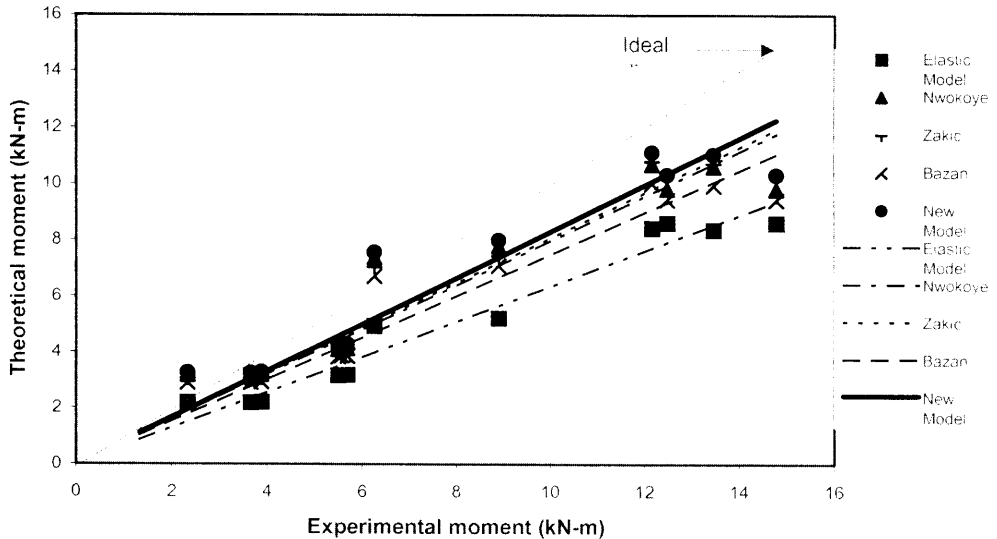


Figure 7: Comparison stress models using theoretical and experimental moments

## 5. Conclusions

A modified stress model for timber beams based on the previous existing models and principle of plasticity was developed. The following conclusions are drawn,

- a) A new theoretical stress model for the prediction of the ultimate strength of tropical hardwood timber beams is proposed. It is simply expressed in terms of elastic moment ( $M_{elastic}$ ) and moment coefficient ( $\psi$ ), which is a function of strength ratio ( $n$ ) of the beam material.
- b) The proposed model predicts the ultimate bending strength of structural sized specimens of Dark Red Meranti (DRM) timber beams better than the existing stress models.
- c) The distribution of strain across the beam depth at mid span of timber beams is linear at all stages of loading up to near failure condition. The position of neutral axis remains at the mid-depth of the timber beam up to the proportional limit, beyond which it moves towards the tension side as a result of stress redistribution until the beam fails.
- d) The strength ratio ( $n$ ) of ultimate tensile strength ( $F_{tu}$ ) to ultimate compressive strength ( $F_{cu}$ ), obtained from direct tension and compression tests of structural sized timber specimens was greater than 1.
- e) The mean values of the modulus of elasticity (MOE) for tension and compression fibres of the beams are approximately the same and the mean MOE in axial tension is approximately equal to the mean MOE in axial compression.

## Nomenclature

$b$	= width of the beam cross-section
$C$	= internal compressive force on the cross-section of the beam
$c$	= strength reduction factor for the compression stress block ( $c < 1$ )
$E_C$	= modulus of elasticity for extreme compression fibres of the beam
$E_T$	= modulus of elasticity for extreme tension fibres of the beam
$F_{cu}$	= ultimate compressive strength of the beam material obtained from compression tests
$F_{pl}$	= proportional limit stress of the beam
$F_t$	= maximum tensile stress in extreme tension fibres of the beam
$F_{tu}$	= ultimate tensile strength of the beam material obtained from tension tests
$h$	= depth of the beam cross-section
$m$	= slope of the falling branch of the modified compression stress-strain curve in Buchanan's stress model
$M_{elastic}$	= elastic bending moment capacity of the beam
$M_u$	= ultimate bending moment capacity of the beam

$n$	= the strength ratio or the ratio of ultimate tensile strength to ultimate compressive strength of the beam material ( $n = F_{tu}/F_{cu}$ and $n > 1$ )
$T$	= internal tensile force on the cross-section of the beam
$\alpha$	= position factor of compressive stress block measured from the compression edge of the beam
$\beta$	= position factor of compressive stress block measured from neutral axis
$\gamma$	= neutral axis position factor of the beam measured from the tension edge
$\gamma_{pl}$	= neutral axis position factor of the beam at proportional limit
$\gamma_u$	= neutral axis position factor of the beam at ultimate load
$\varepsilon_c$	= compressive strain of beam fibres at proportional limit
$\varepsilon_c$	= maximum compressive strain at extreme fibre in Bazan's stress model
$\varepsilon_o$	= compressive strain at proportional limit stress in Bazan's stress model
$\varepsilon_T$	= tensile strain of beam fibres at proportional limit
$\varepsilon_{TU}$	= maximum tensile strain of beam fibres at ultimate load
$\psi$	= moment coefficient of stress models

## References

- American Society for Testing and Materials (1992) Standard methods of static tests of timbers in structural sizes. *Annual book of ASTM Standards*, D 198-84, 4(9).
- American Society for Testing and Materials (1992) Standard test methods for specific gravity of wood and wood-based materials. *Annual book of ASTM Standards*, D 2395-83, 4(9).
- American Society for Testing and Materials (1992) Standard test methods for direct moisture content measurement of wood and wood-based materials. *Annual book of ASTM Standards*, D 4442-92, 4(9).
- Bazan, I. M. M. (1980) *Ultimate Bending Strength of Timber Beams*. Ph.D. Dissertation, Nova Scotia Tech. College, Halifax.
- Buchanan, A. H. (1990) Bending strength of lumber. *Journal of Structural Engineering (ASCE)*, 116(5): 1213-1229.
- Choo, K. T. and Lim, S. C. (1983) *Malaysian timbers: Dark red meranti*. Malaysian Forest Service Trade Leaflet, Ministry of Primary Industry, Malaysia.
- Khin M. Z. (2002) *An Evaluation of Ultimate Strength and the Performance of Timber Beams*. M. Eng. Thesis, Universiti Teknologi Malaysia.
- Malhotra, S. K. and Bazan, I. M. M. (1980) Ultimate bending strength theory for timber beams. *Wood Science*, 12(7): 50-63.
- Moe, J. (1961) The mechanism of failure of wood in bending. *Publication International Association for Bridge & Structural Engineering*, 21: 163-178.
- Nwokoye, D. N. (1972) *An Investigation into an Ultimate Beam Theory for Rectangular Timber Beams – Solid and laminated*. Timber Research and Development Association (TRADA).
- Standard and Industrial Research Institute of Malaysia (SIRIM) (2001) *Code of practice for structural use of timber: Part 2: Permissible stress design of solid timber*. MS 544: Part 2: 2001.
- Zakic, B. D. (1973) Inelastic bending of wood beams. *Journal of the Structural Division (ASCE)*, 99(10): 2079-2095.